Vertically Integrated Modeling of Light-Induced Defects: Process Modeling, Degradation Kinetics and Device Impact

Hannu S. Laine[1], Henri Vahlman[1], Antti Haarahiltunen[1], Mallory A. Jensen[2], Chiara Modanese[1], Matthias Wagner[3], Franziska Wolny[3,4], Tonio Buonassisi[2] and Hele Savin[1,a]

[1]*Department of Electronics and Nanoengineering, Tietotie 3, Aalto University, 02150 Espoo, Finland*
[2]*Massachusetts Institute of Technology, 77 Massachusetts Avenue, Cambridge, 02139 MA, USA*
[3]*SolarWorld Industries GmbH, Martin-Luther-King-Str. 24, 53175 Bonn, Germany*
[4]*Currently at Fraunhofer Institute for Photonic Microsystems IPMS, Maria-Reiche-Str. 2, 01109 Dresden, Germany*

[a]Corresponding author: hele.savin@aalto.fi

Abstract. As photovoltaic (PV) device architectures advance, they turn more sensitive to bulk minority charge carrier lifetime. The conflicting needs to develop ever advancing cell architectures on ever cheapening silicon substrates ensure that various impurity-related light-induced degradation (LID) mechanisms will remain an active research area in the silicon PV community. Here, we propose vertically integrated defect modeling as a framework to accelerate the identification and mitigation of different light induced defects. More specifically, we propose using modeled LID-kinetics to identify the dominant LID mechanism or mechanisms within complete PV devices. Coupling the LID-kinetics model into a process model allows development of process guidelines to mitigate the identified LID-mechanism within the same vertically integrated simulation tool. We use copper as an example of a well-characterized light-induced defect: we model the evolution of copper during solar cell processing and light soaking, and then map the deleterious lifetime effect of Cu-LID onto device performance. We validate our model using intentionally Cu-contaminated material processed on an industrial PERC-line and find that our model reproduces the LID-behavior of the manufactured solar cells. We further show via simulations that Cu-LID can be mitigated by reducing the contact co-firing peak temperature, or the cooling rate after the firing process.

INTRODUCTION

Silicon solar cells and modules suffer from various kind of light-induced degradation (LID) mechanisms. Particularly new device architectures, such as the Passivated Emitter and Rear Cell (PERC) architecture [1-3] or new substrate materials, such as quasimono-silicon [4], may expose previously robust solar cell processes to LID. Since different LID-mechanisms have different root causes and thus different mitigation strategies, it is imperative to rapidly identify the dominant LID-mechanism operating in industrial PV devices. The investigation into the root cause of observed LID phenomena often leverages lifetime samples, whether in the form of lifetime spectroscopy [5-9] or analysis of LID kinetics [10-16]. While these techniques can ultimately reach their goal, the manufacture of lifetime samples is not technically necessary to manufacture functioning solar panels, and thus these techniques may require the adoption of non-essential processing and characterization tools.

Here, we seek to accelerate the identification and mitigation of different LID mechanisms in an industrial environment. Specifically, we investigate whether LID-mechanisms could be identified via simulations based on the degradation behavior of complete devices and whether vertically integrating a LID-model and a process model could be used to develop process guidelines to mitigate the identified LID-defect in the same simulation environment. We use Cu-related LID (Cu-LID) as an example of a reasonably well-understood LID-mechanism [17].
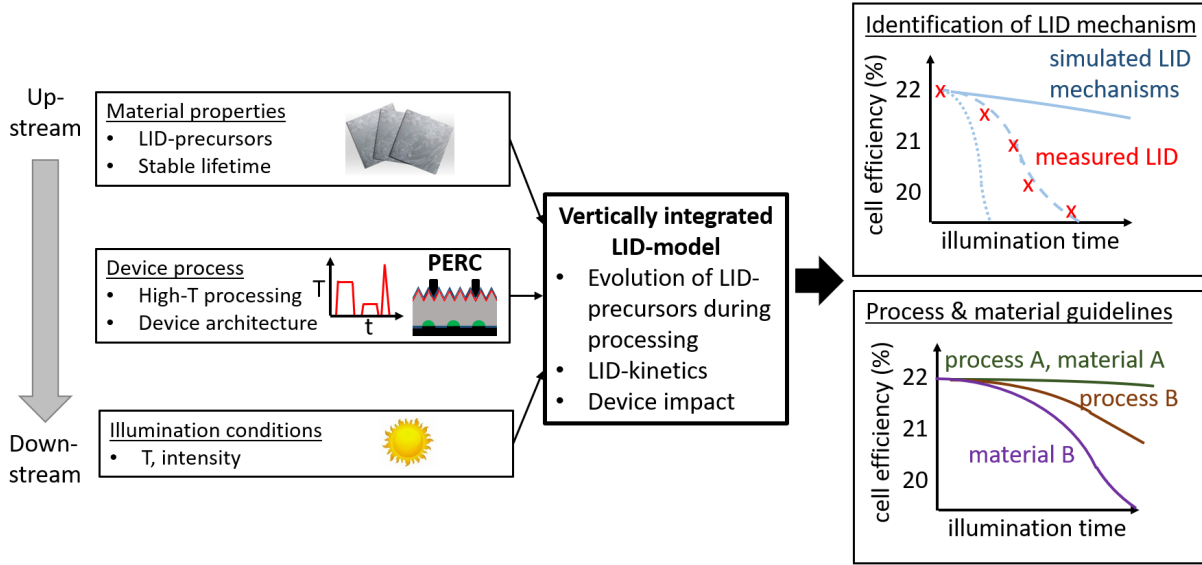
FIGURE 1. A schematic of the vertically integrated LID-model.

VERTICALLY INTEGRATED LID-MODEL: EXAMPLE OF CU-LID

Vertically integrated LID-model refers to a comprehensive LID model, which uses as input the LID-relevant parameters across the full solar cell lifespan beginning from upstream material properties and continuing on to device process and architecture details, as well as illumination conditions of complete devices. Fig. 1 presents a schematic of such a model. The model can then be used to reproduce LID-curves that can be used as an identification tool for the dominant LID-mechanisms, as well as map how the LID-behavior evolves with different materials, processes or device architectures. Here, we present an example of such a model for Cu-LID.

The central physical process of Cu-LID is the precipitation of benign interstitial copper point defects into recombination active Cu silicide precipitates under carrier injection [17]. The injection-dependent lifetime impact of these precipitates is modeled using a Schottky junction model for metallic precipitates [18]. The precursors for Cu-LID are thus Cu point defects, and our model inputs include the initial Cu point defect concentration $[Cu]_{init}$ as well as the stable lifetime that does not vary with illumination time $\tau_{non-LID}$. The LID-kinetics model used here is extensively described in [17] and experimentally validated in [19]. The impact of lifetime onto device efficiency is modeled by using the bulk lifetime and injection-dependent efficiencies modelled for a PERC-device with an architectural efficiency limit of 21.5% [20], i.e., the modeled efficiency of the device is 21.5% given an infinite bulk lifetime.

During device processing, the bulk Cu point defect concentration varies due to diffusion of copper point defects from the bulk into the heavily-doped phosphorus emitter, and vice versa. We numerically model the diffusion of copper accounting for the temperature-dependent diffusivity and solubility of Cu with the algorithm described by Hieslmair *et al.* [21]. As the local solubility of Cu is heavily dependent on the local phosphorus concentration, we also model the phosphorus in-diffusion from a POCl$_3$ source using the model proposed by Bentzen et al. [22] and assuming a 3×10^{20} cm^{-3} surface phosphorus concentration [23]. The specific expressions for the temperature-dependent Cu solubility as a function of phosphorus doping in the emitter and boron doping in the bulk are taken from [24] and [17], respectively. The impact of boron-copper pairing on the diffusivity of copper is modeled as in [25]. Within the phosphorus layer, the gettered copper is assumed immobile, and the diffusivity is thus:

$$D_{Cu} = \frac{D_{Cu,int}}{k_{seg}},$$

where $D_{Cu,int}$ is the diffusivity of Cu in intrinsic silicon [25] and k_{seg} is the local segregation coefficient, *i.e.,* the ratio of Cu solubility in the phosphorus-doped emitter and in the bulk.
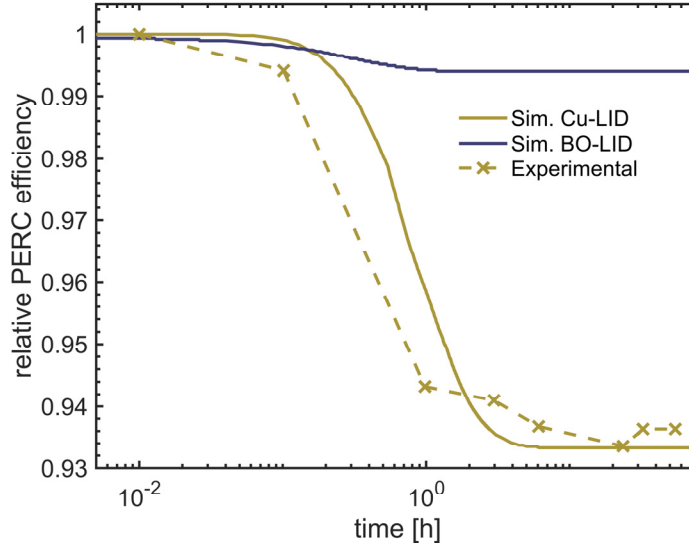
FIGURE 2. The LID behavior of Cu-contaminated Cz-PERC cells compared to modeled Cu-LID and BO-LID behavior. The illumination intensity was 0.5 suns and temperature 75°C.

IDENTIFICATION OF DOMINANT LID MECHANISMS FROM DEVICE DEGRADATION

The first step of LID-mitigation is identifying the dominant LID-mechanism. As a proof of concept for our modeling approach, we use Cz-substrates intentionally contaminated with Cu processed into PERC devices. Details of the contamination process and device results can be found in [26]. We use the background lifetime, i.e., the lifetime limit imposed by defects besides the modeled light-induced defects, as a simulation parameter to match the initial efficiency (absolute efficiencies not shown due to confidentiality). For this study, Cz-substrates with a high density ($\sim 4 \times 10^5$ cm^{-2}) of bulk microdefects (BMD) were used to sensitize the devices for Cu-LID [27]. Because the BMD's also limit the background lifetime, the lifetime value used here is 7 µs. On the other hand, [Cu$_i$] before illumination (after the complete device process) is fixed to 8×10^{13} cm^{-3} such that the simulated total degradation matches the experimentally observed degradation. Similar Cu concentrations have been observed at solar-grade feedstock material [7] and process lines [4].

For comparison, we also simulated the expected BO-kinetics, using the parametrization used by Schön et al. [28] for compensated n-type silicon that was also recently used by Vahlman *et al.* for p-type silicon [19] The parametrization is based on the so called fast and slow recombination centers (FRC and SRC, respectively), with their properties modeled as in [29-32]. The used boron and interstitial oxygen concentrations were $7 \cdot 10^{15}$ cm^{-3} and $9.5 \cdot 10^{17}$ cm^{-3}, respectively, as measured from the as-grown wafers prior to cell processing [26].

Fig. 2 demonstrates that the simulated Cu-LID degradation curve reproduces the precipitous efficiency drop at approximately 1 h observed in the experimental devices, hence implying Cu-LID to be the dominant LID mechanism in the cells. In contrast, the simulated BO-LID is a less suitable candidate for the main LID-mechanism, because the modeled simulation extent is less than 1%$_{rel}$, although the experimentally observed degradation is approximately 7%$_{rel}$. Note that the [B] and [O$_i$] values used were chosen to be the highest values within the measurement uncertainty [26], suggesting that the actual BO-LID is more likely to be less than more severe than what simulated here.

SIMULATION-INFORMED PROCESS GUIDELINES TO MITIGATE CU-LID

Next, we couple the LID-model into the process model and draw guidelines to mitigate Cu-LID. The simulation parameters and results are summarized in Fig. 3. The simulated starting material contains [Cu]$_{init}$ of 8.3×10^{13} cm^{-3}, spread homogeneously in the as-grown wafer, similarly as recently found in LID-affected silicon [7], as well as a 1
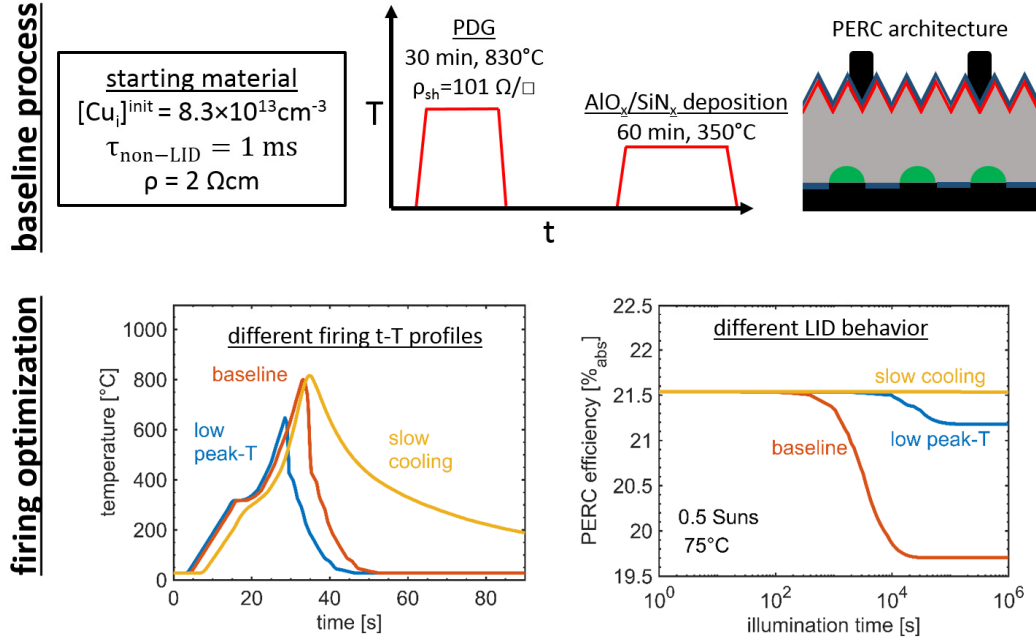
FIGURE. 3. Firing time-temperature profile optimization for PERC devices to mitigate Cu-LID via vertically integrated LID-modeling. The top row shows the baseline process parameters, which are held constant at all simulations. The bottom left figure shows the three different firing time-temperature profiles simulated and the bottom right figure shows the resulting simulated LID-curves.

ms background lifetime. The simulated cell architecture is the PERC device described in [20] and the thermal processing includes a typical 30 min, 830°C phosphorus diffusion step resulting in an approximately 100 $\Omega/\square$ emitter followed by an AlO$_x$ / SiN$_x$ deposition for 60 minutes at 350°C. For contact co-firing, we investigate three different time-temperature profiles. The baseline profile involves a high temperature (>800°C) peak with fast cooling (~100°C/s), whereas the alternative profiles include either a lower peak temperature (~650°C) or a slow cooling rate (10−20°C/s). The simulated LID-curves show that the baseline profile shows LID of up to approximately 2 %$_{abs}$, whereas both of the alternative profiles significantly reduce LID, with the slow cooling profile being more effective. The physical mechanism behind LID-response of the different firing profiles is out-diffusion of gettered copper from the emitter back to the bulk during firing [33]. An experimental verification of this mechanism has been completed on reference lifetime samples and will be published in a separate study [34].

CONCLUSIONS AND OUTLOOK

We presented a novel modeling framework, called vertically integrated LID modeling, to accelerate the identification and mitigation of different light induced defects in commercial crystalline silicon solar cells. We used Cu-LID as a well-characterized light-induced defect to validate our approach by modeling the LID-behavior of intentionally Cu-contaminated Cz-PERC solar cells. We further drew process guidelines via simulations to mitigate Cu-LID. Specifically, we showed that Cu-LID can be mitigated by reducing the contact co-firing peak temperature, or the cooling rate after the firing process.

While the present study focused largely on Cu-LID, there are other examples of light-induced defects that are well-understood that could be coupled into a similar simulation tool, such as: the boron-oxygen (BO) complex [14,16,28-32] and Fe-B pair-dissociation [35]. While this approach is not directly applicable to light-induced defects without an established physical root cause, such as the so called Light and Elevated Temperature Induced Degradation (LeTID) [1-3], this approach can be used to rule out root causes of unknown LID phenomena, and thus help concentrate research efforts elsewhere.

ACKNOWLEDGMENTS

REFERENCES

1. F. Kersten, P. Engelhart, H.-C. Ploigt, A. Stekolnikov, T. Lindner, F. Stenzel, M. Bartzsch, A. Szpeth, K. Petter, J. Heittman, and J. W. Müller, Sol. Energy Mat. Sol. Cells **142**, 83 - 86 (2015).
2. M. Padmanabhan, K. Jhaveri, R. Sharma, P. Kanti Basu, S. Raj, J. Wong, and J. Li, Rrl Solar **10**, pp. 874 – 881 (2016).
3. T. Luka, S. Großer, C. Hagendorf, K. Ramspeck, and M. Turek, Sol. Energy Mater. Sol. Cells **158**, pp. 43 – 49 (2016).
4. H. Vahlman, M. Wagner, F. Wolny, A. Krause, H. Laine, A. Inglese, M. Yli-Koski, H. Savin, Phys. Status Solidi A **214**, 1700321 (2017).
5. K. Nakayashiki, J. Hofstetter, A. E. Morishige, T.-T. A. Li, D. Berney Needleman, M. A. Jensen, T. Buonassisi, IEEE J. Photov. **6**, p. 860 – 868 (2016).
6. D. Chen, M. Kim, B. V. Stefani, B. J. Hallam, M. D. Abbot, C. E. Chan, R. Chen, D. N. R. Payne, N. Nampalli, A. Ciesla, T. H. Fung, K. Kim, and S. R. Wenham, Sol. Energy Mat. Sol. Cells **172**, p. 293 – 300 (2017).
7. T. Niewelt, F. Schindler, W. Kwapil, R. Eberle, J. Schön, and M. C. Schubert, Prog. Photov. *in press*.
8. C. Vargas, Y. Zhu, G. Coletti, C. Chan, D. Payne, M. Jensen, and Z. Hameiri, Appl. Phys. Lett. **110**, p. 092106 (2017).
9. D. Bredemeier, D. Walter, S. Herlufsen, and J. Schmidt, AIP Advances **6**, p. 035119 (2016).
10. C. E. Chan, D. N. R. Payne, B. J. Hallam, M. D. Abbot, T. H. Fung, A. M. Wehnam, B. S. Tjahjono, S. R. Wenham, IEEE J. Photov. **6**, p. 1473 – 1479 (2016).
11. W. Kwapil, T. Niewelt, and M. C. Schubert, Sol. Energy Mat. Sol. Cells **173**, p. 80 – 84 (2017).
12. A. Inglese, J. Lindroos, H. Vahlman, and H. Savin, J. Appl. Phys. **120**, p. 125703 (2016).
13. N. Nampalli, T. H. Fung, S. Wenham, B. Hallam, and M. Abbot, Frontiers in Energy **11** (2017).
14. A. Herguth, G. Hahn, J. Appl. Phys. **108**, p. 114509 (2010).
15. D. Bredemeier, D. Walter, and J. Schmidt, Sol. Energy Mater. Sol. Cells **173**, pp. 2-5 (2017).
16. B. Hallam, M. Abbot, J. Bilbao, P. Hamer, N. Gorman, M. Kim, D. Chen, K. Hammerton, D. Payne, C. Chan, N. Nampalli, and S. Wenham, Energy Procedia **92**, pp. 42-51 (2016).
17. H. Vahlman, A. Haarahiltunen, W. Kwapil, J. Schön, A. Inglese, and H. Savin, J. App. Phys. **121**, p. 195703 (2017).
18. W. Kwapil, J. Schön, W. Warta, and M. C. Schubert, IEEE J. Photov. **5**, p. 1285 – 1292 (2015).
19. H. Vahlman, A. Haarahiltunen, W. Kwapil, J. Schön, A. Inglese, and H. Savin, J. Appl. Phys. **121**, p. 195704 (2017).
20. J. Hofstetter, C. del Cañizo, H. Wagner, S. Castellanos, and T. Buonassisi, Prog. Photov. **24**, p. 122 – 132 (2016).
21. H. Hieslmair, S. Balasubramanian, A. A. Istratov, and E. R. Weber, Semicond. Sci. Technol. **16**, p. 567 (2001).
22. A. Bentzen, A. Holt, J. S. Christensen, and B. G. Svensson, J. Appl. Phys. **99**, p. 064502 (2006).
23. J. Hofstetter, D. P. Fenning, M. I. Bertoni, J. F. Lelièvre, C. del Cañizo, and T. Buonassisi, Prog. Photov. **19**, p. 487 – 497 (2011).
24. R. Hoelzl, D. Huber, K.-J. Range, L. Fabry, J. Hage, and R. Wahlich, J. Electrochem. Soc. **147**, p. 2704 – 2710 (2000).
25. A. A. Istratov, C. Flink, H. Hieslmair, E. R. Weber, and T. Heiser, Phys. Rev. Lett. **81**, p. 1243 – 1246 (1998).
26. C. Modanese, M. Wagner, F. Wolny, A. Oehlke, H. S. Laine, A. Inglese, H. J. Vahlman, M. Yli-Koski, and H. Savin, "Impact of copper on light-induced degradation in Czochralski silicon PERC solar cells," *submitted*.
27. H. Väinölä, M. Yli-Koski, A. Haarahiltunen, and J. Sinkkonen, J. Electrochem. Soc. **150**, p. G790 – G794.
28. J. Schön, T. Niewelt, J. Broisch, W. Warta, and M. C. Schubert, J. Appl. Phys. **118**, p. 245702 (2016).

29. V. V. Voronkov, R. Falster, K. Bothe, B. Lim, and J. Schmidt, J. Appl. Phys. **110**, p. 063515 (2011).
30. T. Niewelt, J. Schön, J. Broisch, W. Warta, and M. C. Schubert, Phys. Status Solidi RRL **9**, 692 (2015).
31. J. D. Murphy, K. Bothe, R. Krain, V. V. Voronkov, and R. J. Falster, J. Appl. Phys. **111**, 113709 (2012).
32. K. Bothe, R. Sinton, and J. Schmidt. Prog. Photovoltaics: Res. Appl. **13,** 287 (2005).
33. M. A. Jensen, A. E. Morishige, S. Chakraborty, R. Sharma, H. S. Laine, B. Lai, V. Rose, A. Youssef, E. E. Looney, S. Wieghold, J. R. Poindexter, J.-P. Correa-Beana, T. Felisca, H. Savin, J. B. Li, and T. Buonassisi, IEEE J. Photov. **8**, p. 448 – 445 (2018).
34. N. Nampalli, H. S. Laine, J. Colwell, V. Vähänissi, A. Inglese, C. Modanese, H. Vahlman, M. Yli-Koski, and H. Savin, "Rapid thermal anneal activates light induced degradation due to copper redistribution," *submitted*.
35. M. Kim, M. Abbot, N. Nampalli, S. Wenham, B. Stefani, and B. Hallam, J. Appl. Phys. **121**, p. 053106 (2017).